Structural and Dynamic Properties of $OsH_2X_2L_2$ (X = Cl, Br, I; L = P^iPr_3) Complexes: Interconversion between Remarkable Non-Octahedral Isomers

Dmitry G. Gusev,*,†,§ Roger Kuhlman,† Joe R. Rambo,‡ Heinz Berke,*,§ Odile Eisenstein,*,‡ and Kenneth G. Caulton*,†

Contribution from the Department of Chemistry, Indiana University, Bloomington, Indiana 47405-4001, Laboratoire de Chimie Théorique, Bâtiment 490, Université de Paris-Sud, 91405 Orsay, France, and Institute of Inorganic Chemistry, University of Zürich, Winterthurerstrasse 190, 8057 Zürich, Switzerland

Received August 1, 1994[⊗]

Abstract: Proton and ^{31}P NMR data reveal that the molecules $Os(H)_2X_2L_2$ (X = halide, L = P^iPr_3) exist in solution as two rapidly interconverting isomers, one having C_2 symmetry (as seen in the solid-state structure) and one having no symmetry. Three distinct intramolecular rearrangements were detected and quantified ($\Delta G^{\ddagger}$), and P/H coupling constants were employed to estimate P−Os−H angles in the nonsymmetric isomer. The geometries of these two isomers were determined at the MP2 level by gradient method with effective core potential *ab initio* calculations. The geometry calculated for the symmetric isomer is a distorted octahedron with C_{2v} symmetry. The solid-state structure, which resembles the calculated symmetric structure, is shown to be the result of opposing forces: steric interactions between phosphine and chlorine ligands and bonding preference of the chlorine ligands. The structure of the nonsymmetric isomer is related to the structure calculated for the symmetric isomer by exchange of one hydride for one chloride together with further slight geometric distortions. Using the calculated structures, physical mechanisms for all observed fluxionality are proposed.

Introduction

The molecule $Os(H)_2Cl_2L_2$ (L = P^iPr_3)[1] is an example of the class of hydride−halide complexes $MH_mX_nL_p$ which we have been investigating recently. While the structure and bonding are now well-understood for d^8-square planar[2] and d^6-five-coordinate[3] complexes, little is known in this regard about d^4-six-coordinate complexes. This molecule is a member of this class, has a 16-valence electron count (ignoring any Cl → Os π-donation), but most remarkably, has a structure significantly distorted from octahedral (it has only C_2 symmetry).[1] The X-ray diffraction view of the molecule (Figure 1) shows cisoid phosphines (∠P−Os−P = 112°), and cisoid chlorides (∠Cl−Os−Cl = 83°) with a dihedral angle of 45.9° between these planes. The hydrides were suggested[1] to be transoid (∠H−Os−H = 148°), bisect the P−Os−P angle, and bend somewhat into the phosphine hemisphere of the molecule. These distortions make this d^4, Os^{IV} complex diamagnetic, in contrast to the $S = 1$ state expected for an octahedral ligand field.

At 25 °C, the molecule exhibits one triplet in the hydride region of the ^1H NMR and a singlet in the $^{31}P\{^1H\}$ NMR spectrum. The structure was originally described as a square antiprism with two vacant coordination sites. For the purpose of describing the fluxional processes observed by NMR studies, it is convenient to consider the structure (Scheme 1) as a distorted tetrahedron (i.e., $OsCl_2P_2$) with the hydrides occupying two PPX (X = Cl) faces. Because of this distortion (i.e., the $OsCl_2$ and OsP_2 planes are not orthogonal), the description as a bicapped tetrahedron (with the hydrides the capping groups) is also imperfect.[4] According to the published X-ray data, there are the following interligand distances (Å): 3.8 (P−P), 3.2 (Cl−Cl), 3.3 and 4.4 (P−Cl).

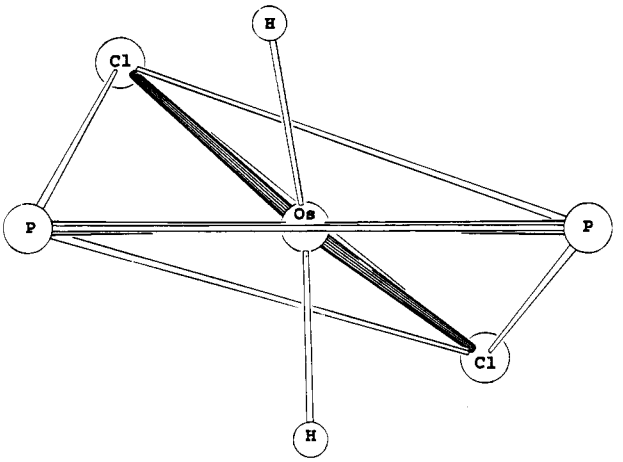

Figure 1. ORTEP drawing of the inner coordination sphere of $Os(H)_2Cl_2(P^iPr_3)_2$, viewed edge-on to the OsP_2 plane. This shows clearly the twist of the $OsCl_2$ plane away from coplanarity with or orthogonality to the OsP_2 plane. Lines connecting P and Cl atoms are not bonds, but illustrate the distorted heavy atom polyhedron.

† Indiana University.
‡ Université de Paris-Sud.
§ University of Zürich.
⊗ Abstract published in *Advance ACS Abstracts,* December 15, 1994.

(1) Aracama, M.; Esteruelas, M. A.; Lahoz, F. J.; Lopez, J. A.; Meyer, U.; Oro, L. A.; Werner, H. *Inorg. Chem.* **1991**, *30*, 288.
(2) Huheey, S. E. *Inorganic Chemistry*, 3rd ed., 1983, p 409.
(3) Rachidi, I. E.-I.; Eisenstein, O.; Jean, Y. *New J. Chem.* **1990**, *14*, 671. Riehl, J.-F.; Jean, Y.; Eisenstein, O.; Pélissier, M. *Organometallics* **1992**, *11*, 729. Albinati, A.; Bakhmutov, V. I.; Caulton, K. G.; Clot, E.; Eckert, J.; Eisenstein, O.; Gusev, D. G.; Grushin, V. V.; Hauger, B. E.; Klooster, W. T.; Koetzle, T. F.; McMullan, R. K.; O'Loughlin, T. J.; Pélissier, M.; Ricci, J. S.; Sigalas, M. P.; Vymenits, A. B. *J. Am. Chem. Soc.* **1993**, *115*, 7300. Poulton, J. T.; Sigalas, M. P.; Folting, K.; Streib, W. E.; Eisenstein, O.; Caulton, K. G. *Inorg. Chem.* **1994**, *33*, 1476. Bickford, C. C.; Johnson, T. J.; Davidson, E. R.; Caulton, K. G. *Inorg. Chem.* **1994**, *33*, 1080. Hauger, B. E.; Gusev, D. G..; Caulton, K. G. *J. Am. Chem. Soc.* **1994**, *116*, 208. Poulton, J. T.; Sigalas, M. P.; Eisenstein, O.; Caulton, K. G. *Inorg. Chem.* **1993**, *32*, 5490.
(4) Hoffmann, R.; Howell, J. M.; Rossi, A. M. *J. Am. Chem. Soc.* **1976**, *98*, 2484.

0002-7863/95/1517-0281$09.00/0

Scheme 1

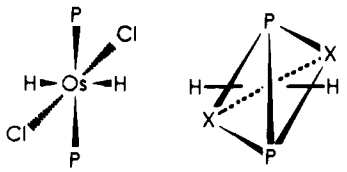

Several interesting reactions have been reported for this molecule, including formation of η^2-H_2 complexes, either upon addition of H_2 or even on addition of Lewis base.[5,6] The molecule has also been demonstrated to catalyze the reduction of olefins and of ketones. We felt that it would be valuable to try to understand its unusual solid-state structure and its fluxionality, as a tool for understanding its reactivity. In fact, the present study has revealed unusually complex behavior, including a rare case where two structural isomers of a dihydride are detectable, and where one isomer has inequivalent hydrides. Furthermore, in the course of this investigation, a surprising method of halide exchange at a hydride-containing metal has been observed, via reaction with methyl iodide. A full description of this halide exchange reaction is presented here, including kinetic data and mechanistic interpretations.

Experimental Section

General. All manipulations were performed under inert atmosphere or *in vacuo* using standard Schlenk and glovebox techniques. All glassware was flame dried under vacuum prior to use. Solvents (including MeI and EtBr) were dried, distilled, and stored in bulbs with Teflon valves. Microanalyses were performed by Oneida Research Services. IR spectra were recorded on a Nicolet 510P FT-IR spectrometer. NMR spectra were obtained on either a Bruker 500 MHz, a Nicolet 360 MHz, or a Varian 300 MHz instrument, with chemical shifts referenced to residual solvent peaks (^{1}H) or external H_3PO_4 (neat, ^{31}P). $OsH_2Cl_2(P^iPr_3)_2$ was synthesized according to the literature.[1] The mixture of $CDFCl_2/CDF_2Cl$ was synthesized by the method of Siegel,[7] stored under vacuum in a Teflon-sealed glass bulb in a −20 °C freezer, and vacuum transferred into NMR tubes, which were flame sealed before use. Trimethylsilyl reagents were used as received (Aldrich) and stored in glass bulbs with Teflon closures. Methyl-d_3 iodide was used as received (Cambridge Isotope Laboratories).

$OsH_2I_2(P^iPr_3)_2$. Method I: A Schlenk flask was charged with $OsH_2Cl_2(P^iPr_3)_2$ (100 mg, 0.17 mmol). MeI (5 mL, 80.3 mmol) was then added and the solution was stirred for 18 h, after which the color had changed from light brown to violet. Removal of volatiles *in vacuo* yielded $OsH_2I_2(P^iPr_3)_2$ quantitatively. ^{31}P{^{1}H} NMR ($CDCl_3$, 20 °C): 45.8 (s). ^{1}H NMR ($CDCl_3$, 20 °C): 2.21 (m, 6H), 1.33 (dd, J_{HP} = 15.0 Hz, J_{HH} = 7.5 Hz, 36H), −12.44 (t, J_{HP} = 32.1 Hz, 2H). IR (KBr): ν_{Os-H} = 2186, 2174 cm^{-1}. Anal Calcd: C, 28.31; H, 5.57. Found: C, 28.21; H, 5.79. **Method II:** In a Schlenk flask, $OsH_2Cl_2(P^iPr_3)_2$ (150 mg, 0.26 mmol) was dissolved in CH_2Cl_2 (10 mL). With constant stirring, an excess of Me_3SiI (200 μL, 0.71 mmol) was added. After a few minutes, the color had changed to violet. After an additional 20 min of stirring, the volatiles were removed *in vacuo*, quantitatively yielding $OsH_2I_2(P^iPr_3)_2$.

$OsH_2Br_2(P^iPr_3)_2$. The dibromide compound can be synthesized by Method I or II, using EtBr (stirring for 1 week) or Me_3SiBr in CH_2Cl_2 (20 min). ^{31}P{^{1}H} NMR ($CDCl_3$, 20 °C): 46.2 (s). ^{1}H NMR ($CDCl_3$, 20 °C): 2.27 (m, 6H), 1.31 (dd, J_{HP} = 14.4 Hz, J_{HH} = 7.2 Hz, 36H), −14.89 (t, J_{HP} = 33.7 Hz). IR (KBr): ν_{Os-H} = 2199, 2181 cm^{-1}. Anal Calcd: C, 32.15; H, 6.59. Found: C, 32.38; H, 6.55.

Radical Inhibition Experiment. In a drybox, one NMR tube was charged with 2,6-di-*tert*-butyl-4-methylphenol, BHT (20.0 mg, 0.091 mmol). In a glass vial, $OsH_2Cl_2(P^iPr_3)_2$ (22.0 mg, 0.0377 mmol) was dissolved in CD_3I (680 μL). Approximately half of the solution was then added to the NMR tube containing BHT, and the other half was added to a separate NMR tube. Both tubes were capped, and the reactions were monitored by integration of the hydride resonances in ^{1}H NMR, at approximately 60-min intervals. When not in the NMR probe, the tubes were stored together at ambient temperature.

Kinetic Analysis of Reaction with CD_3I. $OsH_2Cl_2L_2$ (10.0 mg, 0.0171 mmol) was weighed into an NMR tube. CD_3I (400 μL) was added via syringe. The reaction was followed by integration of hydride signals in ^{1}H NMR. The tube remained in the probe at a constant temperature of 28.8 °C.[8] Spectra were taken at time intervals over which significant changes in composition were observed (about 1 per min initially, and about 1 per h at the end of the kinetic run). The total concentration, ['Cl_2'] + ['ClI'] + ['I_2'], was assumed to remain constant at 0.0429 mol/L throughout the experiment. The reaction in C_6D_6:CD_3I (1:1) was studied analogously.

Computational Method. An effective core potential (ECP) was used for Os, Cl, and P. For Os, the relativistic ECP of Christiansen et al. that includes the 5s and 5p electrons in the valence shell was chosen[9] along with a (7s7p6d) Gaussian basis set contracted into [3211/421/411] for the valence shell. For Cl and P, (4s4p) Gaussian basis sets contracted into [31] with the ECP of Barthelat, et al.[10] for Cl and into [31/31] with the ECP of Stevens and Basch[11] for P were selected. Both Cl and P basis sets also included (5d/1d) polarization functions to avoid earlier problems with unreasonable calculated metal−ligand bond lengths found when polarization functions were absent.[12] For hydrogen atoms bonded directly to the metal center, a (5s) Gaussian basis set of Huzinaga[13] contracted into a [311] basis set and augmented by a (4p/1p) polarization function was used. For all other H atoms (i.e., those of PH_3), a (4s/1s) basis set was chosen.[14]

Calculations presented here were performed at the RHF/MP2 level, as polyhydrides have been properly calculated at this level.[15] When test calculations showed equivalent results, RHF level calculations were performed instead of RHF/MP2 level calculations.[15a] Structural parameters were optimized by the gradient method at either the RHF or RHF/MP2 level with the Gaussian92 set of programs.[16] During optimization, the phosphine ligands, modeled by PH_3, were not allowed to rotate, and the Os−P−H angles and P−H distances were held at fixed values of 118.0° and 1.42 Å, respectively. Unless stated otherwise, all other structural parameters were optimized. Molecular mechanics calculations were performed using Chem3D.

Results

Synthesis of $OsH_2Br_2(P^iPr_3)_2$ and $OsH_2I_2(P^iPr_3)_2$. For $OsH_2Cl_2(P^iPr_3)_2$ ('Cl_2'), an efficient method for halide exchange has been developed which, in the presence of metal hydrides, has no precedent, to our knowledge. Simply dissolving 'Cl_2' in MeI converts the compound to 'I_2' after stirring overnight. 'Cl_2' reacts analogously with EtBr to form 'Br_2', although very long reaction times (>1 week) are needed for complete

(5) Esteruelas, M. A.; Oro, L. A.; Ruiz, N. *Inorg. Chem.* **1993**, *32*, 3793. Esteruelas, M A.; Lahoz, F. J.; Oro, L. A.; Oñate, E.; Ruiz, N. *Inorg. Chem.* **1994**, *33*, 787. Espuelas, J.; Esteruelas, M. A.; Lahoz, F. J.; Oro, L. A.; Ruiz, N. *J. Am. Chem. Soc.* **1993**, *115*, 4683.

(6) Gusev, D. G.; Kuznetsov, V. F.; Eremenko, I. L.; Berke, H. *J. Am. Chem. Soc.* **1993**, *115*, 5831.

(7) Siegel, J. S.; Anet, F. A. L. *J. Org. Chem.* **1988**, *53*, 2629.

(8) Temperature determined by the separation of peaks in a sample of CH_3OH.

(9) Ross, R. B.; Powers, J. M.; Ermler, W. C.; LaJohn, L. A.; Christiansen, P. A. *J. Chem. Phys.* **1990**, *93*, 6654.

(10) Bouteiller, Y.; Mijoule, C.; Nizam, M.; Barthelat, J. C.; Daudey, J. P.; Pélissier, M.; Silvi, B. *Mol. Phys.* **1988**, *65*, 295.

(11) Stevens, W. J.; Basch, H.; Krauss, M. J. *J. Chem. Phys.* **1984**, *81*, 6026.

(12) Pacchioni, G.; Bagus, P. S. *Inorg. Chem.* **1992**, *31*, 4391.

(13) Huzinaga, S. J. *J. Chem. Phys.* **1970**, *53*, 2823.

(14) Dunning, T. H. *J. Chem. Phys.* **1965**, *42*, 1293.

(15) For examples see: (a) Gusev, D. G.; Kuhlman, R.; Sini, G.; Eisenstein, O.; Caulton, K. G. *J. Am. Chem. Soc.* **1994**, *116*, 2685. (b) Maseras, F.; Li, X.-K.; Koga, N.; Morokuma, K. *J. Am. Chem. Soc.* **1993**, *115*, 10974.

(16) Gaussian 92 Revision B: Frisch, M. J.; Trucks, G. W.; Head-Gordon, M.; Gill, P. M. W.; Wong, M. W.; Foresman, J. B.; Johnson, B. G.; Schlegel, H. B.; Robb, M. A.; Reploge, E. S.; Gomperts, R.; Andres, J. L.; Raghavachari, K.; Binkley, J. S.; Gonzalez, C.; Martin, R. L.; Fox, D. J.; DeFrees, D. J.; Baker, J.; Stewart, J. J. P.; Pople, J. A.; Gaussian, Inc., Pittsburgh, PA, 1992.

conversion (eq 1).

$$OsH_2Cl_2L_2 \xrightarrow[-RCl]{RX} OsH_2ClXL_2 \xrightarrow[-RCl]{RX} OsH_2X_2L_2 \quad (1)$$

$$RX = MeI, EtBr; \quad L = P^iPr_3$$

The rate of halide exchange can be drastically increased by using trimethylsilyl reagents. Typically, the bond dissociation energy (BDE) for a C−Cl bond is about 28 kcal/mol greater than BDE(C-I). This difference is greater for silicon−halide bonds: BDE(Si−Cl) − BDE(Si−I) ≈ 35 kcal/mol. This increased driving force appears to accelerate the reaction: halide exchange occurs very rapidly (<20 min), with only a slight excess of Me_3SiI in CH_2Cl_2 solution (eq 2). Reaction with Me_3SiBr is also quite fast (<20 min) for formation of 'Br_2'. Both silyl reagents are inert to further reaction and are sufficiently volatile to be removed *in vacuo* (10^{-2} Torr). Thus, Me_3SiX reagents provide a convenient, reliable, quantitative, and rapid method for conversion of 'Cl_2' to its heavier halide analogs (eq 2).

$$OsH_2Cl_2L_2 \xrightarrow[-Me_3SiCl]{\substack{CH_2Cl_2\\Me_3SiX}} OsH_2ClXL_2 \xrightarrow[-Me_3SiCl]{\substack{CH_2Cl_2\\Me_3SiX}} OsH_2X_2L_2 \quad (2)$$

$$X = Br, I$$

There is a change in color with incorporation of the heavier halides: 'Cl_2' is a yellow-brown solid, 'Br_2' is red, and 'I_2' is violet. All $OsH_2X_2L_2$ are quite soluble in polar aprotic solvents (CH_2Cl_2, THF), poorly soluble in arene or alcohol solvents, and nearly insoluble in ether or pentane. In solution, the compounds are unreactive with water, but they slowly decompose when exposed to oxygen.

Synthesis of $OsH_2XY(P^iPr_3)_2$ (X, Y = Cl, Br, I). If less than 2 equiv of Me_3SiX is reacted with 'Cl_2' or if the reaction of 'Cl_2' with RX is stopped prior to completion, one observes (^1H and ^{31}P NMR) a mixture of three compounds: 'Cl_2', 'X_2', and 'ClX'. Furthermore, if 'X_2' and 'Y_2' are dissolved together, an equilibrium mixture of these and 'XY' quickly forms (eq 3). The facility of this intermetallic halide exchange makes

$$'X_2' + 'Y_2' \overset{K}{\rightleftharpoons} 2'XY' \quad (3)$$

isolation of 'XY' species by solution techniques impossible. However, the hydride resonances are sufficiently resolved for meaningful ^1H NMR studies (see below). We have studied independently similar halide redistribution reactions and proposed a bimolecular mechanism.[17]

Mechanism of the Reaction of $OsH_2Cl_2(P^iPr_3)_2$ with Methyl Iodide. As mentioned before, a C−Cl bond is about 28 kcal/mol stronger than a C−I bond. Little information is available for late transition metal−halide bond strengths,[18] so it is difficult to predict if Os−Cl > Os−I + 28 kcal/mol. However, the reaction in eq 1 is driven by the large excess of MeI present and, perhaps, by evolution of MeCl(g). Therefore, it is not surprising that the reaction occurs even if there is a thermodynamic preference for chloride to remain on osmium, as opposed to carbon.

What is *most* remarkable about this reaction is not the exchange which occurs but the exchange which does *not*. The BDE for C−H is about 15 kcal/mol greater than BDE(C−Cl) (43 kcal/mol > C−I). It is initially quite surprising, then, that reaction with CH_3I does not generate any CH_4. For this reason, we have investigated the mechanism of the reaction.

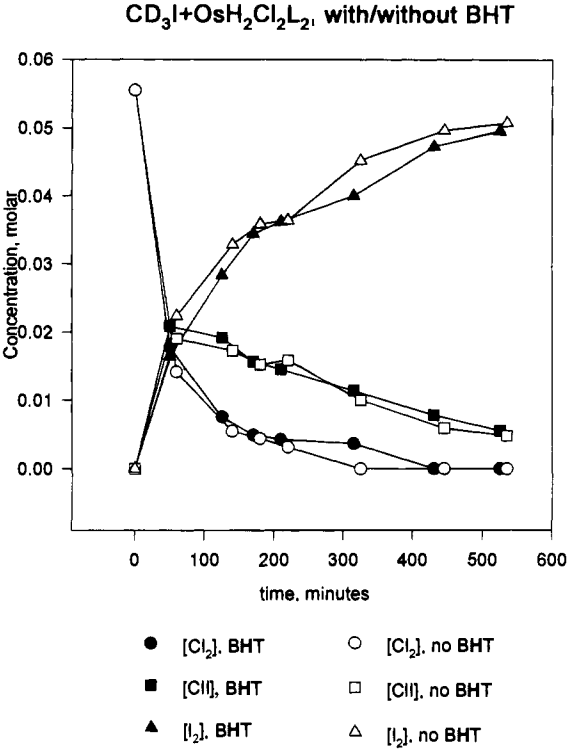

Figure 2. Time evolution of the concentration $Os(H)_2Cl_nI_{2-n}(P^iPr_3)$ ($n = 0-2$) in the presence and absence of the radical scavenger BHT.

Scheme 2

Mechanism I:

$$In + CH_3I \rightleftharpoons In\text{-}I + CH_3\cdot$$

$$[Os]\text{-}Cl + CH_3\cdot \rightarrow CH_3Cl + [Os]\cdot$$

$$[Os]\cdot + MeI \rightarrow [Os]\text{-}I + CH_3\cdot$$

Mechanism II:

$$Os(H)_2Cl_2L_2 + MeI \rightarrow Os(H)_2Cl_2(Me)(I)L_2$$

$$\rightarrow OsH_2ClIL_2 + MeCl$$

Mechanism III:

$$Os(H)_2Cl_2L_2 + MeI \rightarrow \left[L_2H_2ClOs\cdots Cl \;\; I\cdots CH_3\right]^{\ddagger}$$

$$\rightarrow OsH_2ClIL_2 + MeCl$$

Mechanism IV:

$$L_2(H)_2ClOs\text{-}\ddot{Cl} + CH_3\text{-}I \rightarrow \{L_2(H)_2ClOs \leftarrow ClMe^+, I^-\}$$

$$\rightarrow Os(H)_2ClIL_2 + MeCl$$

Radical Mechanism. One explanation of the observed reactivity is a radical mechanism (Mechanism I in Scheme 2, where In is an initiator). However, the rate of the reaction is wholly unaffected by the addition of an excess (>4 equiv) of the known radical scavenger 2,6-di-*tert*-butyl-4-methylphenol (BHT) (see Figure 2), as was determined by following the reaction in CD_3I by ^1H NMR.

(17) Poulton, J. T.; Hauger, B. E.; Kuhlman, R.; Caulton, K. G. *Inorg. Chem.*, accepted for publication.

(18) BDE's (kcal/mol) were determined for Ir−X in the series $IrCl(CO)(PR_3)_2X_2$: Ir−Cl 71(10), Ir−Br 53(5), Ir−I 35(1). See: Blake, D. M. *Coord. Chem. Rev.* **1982**, *47*, 205.

Oxidative Addition–Reductive Elimination. Perhaps the most obvious route for this exchange is oxidative addition of the H_3C-I bond, followed by reductive elimination of H_3C-Cl (Mechanism II, Scheme 2). If the intermediate in this reaction has no hydrogen ligand adjacent to methyl, and subsequent reductive elimination of MeCl is much faster than intramolecular rearrangement, methane formation would not compete. However, this intermediate requires an unusually high oxidation state (VI) and coordination number (8) for osmium.[19]

It is interesting to compare the reaction of 'Cl_2' with CH_3I (eq 1) to those with Me_3SiI (eq 2) and 'I_2' (eq 3). All represent halide exchange reactions of 'Cl_2'. While reaction 1 is relatively slow, reactions 2 and 3 are both quite fast. The main difference in these "reagents" is the presence of a fairly low-energy LUMO for Me_3SiI or 'I_2', which is absent in MeI. This indicates that the Cl transferred must act as a nucleophile at some stage in the reaction and that an electrophilic R in the RI reagent facilitates the exchange.

Four-Centered Transition State. We use the term "four-centered" to describe any transition state (Mechanism III) in which there is some simultaneous bonding between Os–Cl, Cl–C, C-I, and I–Os. Thus, this term implies nothing about the *initial* contact between 'Cl_2' and MeI (either I–Os, Cl–C, or simultaneous). Clearly, this mechanism is consistent with the trend 'I_2', $Me_3SiI \gg MeI$, since donation from chloride to carbon is needed for one of the bonds formed in the transition state.

Nucleophilic Attack. One final mechanistic possibility (Mechanism IV) is attack of bound chloride on carbon, yielding $OsH_2ClL_2(ClMe)^+$ and I^-. Chloromethane could then be displaced by the better nucleophile, I^-, yielding the products. Once again, this mechanism is obviously faster with a more electrophilic reaction partner (Os(16e), Si > C). Alternatively, there could be dissociation of Cl^- from $OsH_2L_2Cl_2(IMe)$. Chloride would then do backside attack at carbon, breaking the C–I bond.

In principle, one could distinguish between Mechanism III and Mechanism IV by reaction of $OsH_2Cl_2L_2$ with an iodocarbon which is stereolabeled at the α position. In this case, the organic product should demonstrate either inversion (outer-sphere halide attack, Mechanism IV) or retention (four-centered transition state, Mechanism III) at that carbon. In fact, *erythro*-neohexyl-*1,2-d*$_2$ iodide was synthesized for this purpose.[20] Unfortunately, reaction of this halocarbon with 'Cl_2' is extremely slow (months in refluxing $CDCl_3$), and the product is not of the form $OsH_2X_2L_2$. We therefore decided to determine the dependence of the reaction rate on solvent polarity. It is well-known that reactions which generate substantial charge separation in the transition state experience tremendous rate enhancements in more polar solvents.[21] For example, the S_N2 reaction, $^nPr_3N + CH_3I \rightarrow {}^nPr_3NCH_3^+ + I^-$ is 50 times faster in EtOH/H_2O (1:1) than in pure EtOH.[22] In order to draw any intelligent conclusions, we first needed to determine reaction rate constants.

Rate Constant Determination and Solvent Dependence.

$$\text{'Cl}_2\text{'} + \text{MeI} \xrightarrow{k} \text{'ClI'} + \text{MeCl} \quad (4)$$

$$\text{'ClI'} + \text{MeI} \xrightarrow{k'} \text{'I}_2\text{'} + \text{MeCl} \quad (5)$$

At first, it would appear that the reactions in eqs 4 and 5 can be analyzed kinetically as a simple case of $A \rightarrow B \rightarrow C$. The tremendous excess of MeI ensures pseudo-first-order conditions and that the reactions are (for all practical purposes) irreversible. However, the system is complicated by the fast equilibrium between 'Cl_2', 'ClI', and 'I_2' (eq 3). Since each spectrum taken provides ['Cl_2'], ['ClI'], and ['I_2'], this equilibrium constant can easily be calculated. K was taken as the average value of ['ClI']^2/['Cl_2']['I_2'] in several measurements, excluding those times where one or more of the concentrations was very low. Knowing K, the system can now be simplified by considering only the total iodide incorporation, called I, which is given by $I = [\text{'ClI'}] + 2[\text{'I}_2\text{'}]$. ['$Cl_2$'], ['ClI'], and ['$I_2$'] can be expressed in terms of I, K, and the total osmium concentration.[23]

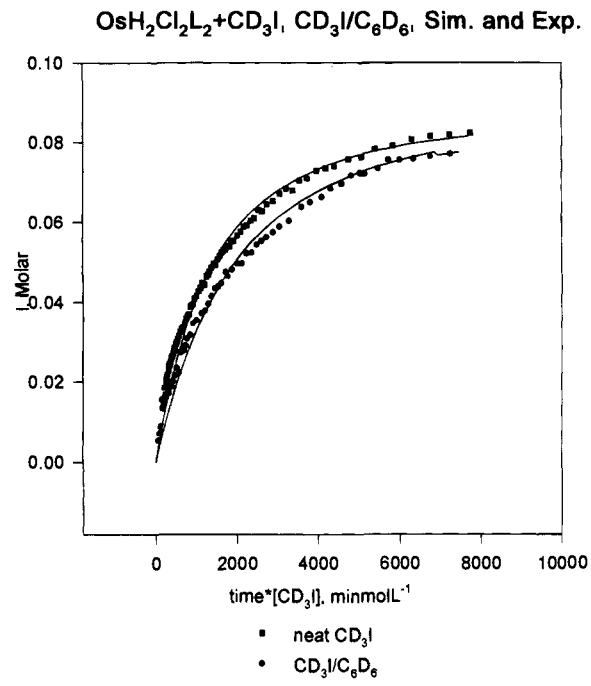

Figure 3. Calculated (line) and observed (solid symbols) iodide incorporation in neat CD_3I and in the mixed solvent $CD_3I + C_6D_6$. See text for rate constants.

Based on the assumptions of mass balance and fast equilibrium, the rate of iodide incorporation, dI/dt, *can* be solved in terms of total osmium concentration, K, k, and k'. However, the function is significantly complex, so that use of the integrated rate expression is not feasible. Therefore, the reaction profile (I *vs* t*[CD_3I], Figure 3) was simulated using the program GEAR[24] and rate constants obtained by "trial-and-error" matching of simulated to experimental data. Data[25] are given for reaction in neat CD_3I ($k = 2.5(2) \times 10^{-5}$ L(mol s), $k' = 3.5(3) \times 10^{-6}$ L/(mol s)), and for CD_3I/C_6D_6 (1:1) ($k = 1.8(3) \times 10^{-5}$ L/(mol s), $k' = 2.8(7) \times 10^{-6}$ L/(mol s)). Since reaction rates are so similar in the two solvent systems of greatly different polarity, we favor the four-centered transition state (Mechanism III).

Possible Transition State Geometry. Halocarbon coordination to Os as a pre-equilibrium step is a reasonable possibility,

(19) We do not consider the possibility of a dihydrogen intermediate, $Os(H_2)Cl_2(Me)(I)P_2$, since H_2 loss would almost certainly be competitive with reductive elimination of MeCl from such a species.

(20) Igau, A.; Gladysz, J. A. *Organometallics* **1991**, *10*, 2327.

(21) Lowry, T. H.; Richardson, K. S. *Mechanism and Theory in Organic Chemistry, 3rd ed.;* 1987; pp 361–367.

(22) Swain, C. G.; Swain, M. S.; Powell, A. L.; Alunni, S. *J. Am. Chem. Soc.* **1983**, *105*, 502.

(23) Details of the calculations are given in the Supplementary Material.

(24) (a) Stabler, R. N.; Chesick, J. *Int. J. Kinet.* **1978**, *10*, 461. (b) McKinney, R. J.; Weigert, F. J. Quantum Chemistry Program Exchange, Program No. QCMP022.

(25) Numbers in parentheses represent deviations which produce noticeably worse fits to experimental data when simulated. There is an additional uncertainty in [CD_3I] for the CD_3I/C_6D_6 mixture, according to the accuracy of the syringes used.

since such reactions are now well-documented,[26] and 'Cl_2' has been shown to coordinate weak ligands.[5] Iodomethane has been established as the most nucleophilic of several halocarbons.[27] Additionally, the vulnerability of MeI to nucleophilic attack has been demonstrated to increase 10^4-10^5-fold when coordinated to a metal.[20,28] X-ray structures have shown the M−I−C angle to be quite acute (102°−107°) in halocarbon complexes.[20,21,29] Assuming an I−Os−Cl bond angle of 76°,[30] and reasonable Os−Cl, Os−I, and I−C bond lengths from X-ray studies, this M−I−C angle gives the transition-state geometry shown in **I**.

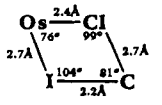

I

The proposed C to Cl distance of 2.7 Å is well within the sum of van der Waals radii. Intermolecular attack at carbon of a metal-bound halocarbon by a metal-bound halide has been reported,[20] and Mechanism III could be considered as an intramolecular version of that reaction.

The observation that k is about seven times greater than k' deserves further comment. Based purely on statistics, one would expect $k = 2k'$ since 'ClI' can undergo degenerate I/I exchange. However, we consider two additional factors to potentially be important: (1) coordination of MeI to 'ClI' is disfavored by the bulkier iodide in comparison to coordination to 'Cl_2', and (2) degenerate I/I exchange is faster than Cl/I exchange due to the greater nucleophilicity of (coordinated) iodide.

NMR Spectral Data. All of the above described dihydrides are easily distinguished at 25 °C in the ^1H NMR spectrum. The absolute values of the hydride chemical shifts and coupling (^2J(H-P)) constants decrease (CD_2Cl_2, 20 °C) as follows: −16.11 ppm/ 34.7 Hz ('Cl_2') > −15.41 ppm/34.0 Hz ('ClBr') > −14.80 ppm/33.6 Hz ('Br_2') > −14.17 ppm/33.4 Hz ('ClI') > −13.61 ppm/32.5 Hz ('BrI') > −12.45 ppm/31.7 Hz ('I_2'). The two phosphines within each molecule show a singlet in $^{31}P\{^1H\}$ NMR (δ *ca.* 45.5)[31] and two resonances in ^1H NMR (δ *ca.* 2.3 and 1.35). The latter (CH_3) is invariably a doublet of doublets (7.2/14.4 Hz) indicating almost zero two-bond P−P coupling ($^2J_{PP} \ll 14.4$ Hz).

Dynamic Averaging of Hydride Chemical Shifts in OsH_2XYL_2. Although observation of a single hydride chemical shift in C_2 symmetric $OsH_2X_2P_2$ (i.e., identical halides) is to be expected, inspection of the structure shown in Scheme 3 predicts two different chemical shifts in OsH_2XYL_2, where the hydrides occupy unlike faces, PPX and PPY. A dynamic process obviously operates in these complexes at room temperature to average the hydride environments. Averaging can be achieved either by (A) hydride or (B) halide physical motion. In case B, a 90° X−Y twist (Scheme 3) represents a satisfactory way to effect exchange between chemical shifts 1 and 2 (a and b label nuclei, while 1 and 2 label environments).

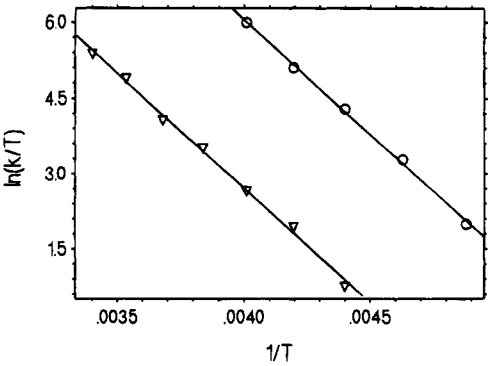

Figure 4. Eyring plot of the site-exchange process shown in Scheme 3 for $Os(H)_2(Cl)(I)(P^iPr_3)_2$, 'ClI' (circles), and for $Os(H)_2(Br)(I)(P^iPr_3)_2$, 'BrI' (triangles).

Scheme 3

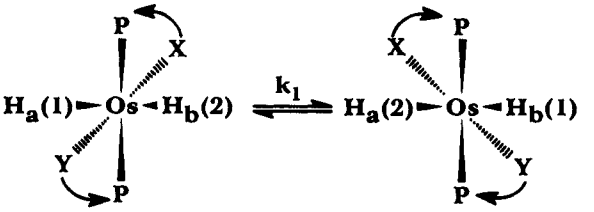

A variable-temperature ^1H NMR study (in CD_2Cl_2) revealed decoalescence of the hydride resonances in OsH_2BrIL_2 and OsH_2ClIL_2 at −35 and −68 °C, respectively. The exchange is faster in OsH_2ClBrL_2, where the slow-exchange limit can only be reached below −85 °C, but multiple spectral changes (see below) complicate that study.

The fact that this decoalescence behavior is a unique feature of OsH_2XYL_2, where $X \neq Y$, is clearly revealed by the ^1H NMR spectra of the equilibrium mixtures. For example, while the hydride resonance of OsH_2BrIL_2 is 300 Hz broad at −35 °C, those for $OsH_2Br_2L_2$ and $OsH_2I_2L_2$ (in the same solution) are well-resolved triplets with line widths of only 4.4 and 3.7 Hz, respectively. The decoalescence of OsH_2XYL_2 species thus involves slowing of a physical motion which does not alter the lifetime of the hydride environment in more symmetric $OsH_2X_2L_2$ species (C_2 ground state structure). Further discussion on this motion will be given in the Computational Studies section.

After decoalescence, two 1:1 resonances of the hydrides experiencing inequivalent environments are observed in OsH_2ClIL_2 (δ −13.68/−15.57) and OsH_2BrIL_2 (δ −13.34/−14.98). Assuming 1:1 two-site exchange, the variable-temperature ^1H NMR spectra were simulated using the DNMR5 program to yield rate constants (k_1) in the temperature range between 20 and −45 °C for OsH_2BrIL_2 and between −25 and −70 °C for OsH_2ClIL_2. The temperature dependence of k_1 presented in an Eyring plot (Figure 4) results in $\Delta H^{\ddagger}$ and $\Delta S^{\ddagger}$ of 9.0 ± 0.2 kcal/mol and 0.8 ± 1 eu in OsH_2ClIL_2 and 9.1 ± 0.2 kcal/mol and −5.5 ± 0.9 eu in OsH_2BrIL_2. These rate data, perhaps, can be better understood if analyzed in terms of the Arrhenius equation, which results in E_a and A of 9.4 kcal/mol and 19.5×10^{12} s^{-1} for OsH_2ClIL_2 and 9.6 kcal/mol and 0.9×10^{12} s^{-1} for OsH_2BrIL_2. These indicate nearly the same barrier heights but different pre-exponential factors. The latter, being larger in the complex with the lighter halide, may reflect higher frequency of attempts to overcome the barrier. We suggest that the strong halide dependence indicates halide motion as the source of the site exchange (Scheme 3).

One important conclusion follows from these observations: in at least two of the dihydrides, OsH_2BrIL_2 and OsH_2IClL_2, there is no fast hydride physical motion between sites 1 and 2

(26) Kulawiec, R. J.; Crabtree, R. H. *Coord. Chem. Rev.* **1990**, *99*, 89. For an example of coordinated trimethylsilyl halide, see: Kirss, R. U. *Inorg. Chem.* **1992**, *31*, 3451.

(27) Winter, C. H.; Veal, W. R.; Garner, C. M.; Arif, A. M.; Gladysz, J. A. *J. Am. Chem. Soc.* **1989**, *111*, 4766.

(28) Burk, M. J.; Segemuller, B.; Crabtree, R. H. *Organometallics* **1987**, *6*, 2241.

(29) Crabtree, R. H.; Gladysz, J. A.; Pathak, D. D.; Adams, H.; White, C. *J. Chem. Soc., Chem. Commun.* **1994**, 733.

(30) That found for Cl−Os−Cl in $[(P^iPr_3)_2H_2Os(\mu\text{-}Cl)_3Os(P^iPr_3)_2H_2]CF_3SO_3$, unpublished results.

(31) Since there is greater dispersion of the hydride than the phosphorus chemical shifts, ^1H NMR is more useful than ^{31}P NMR for detecting certain isomerizations reported here.

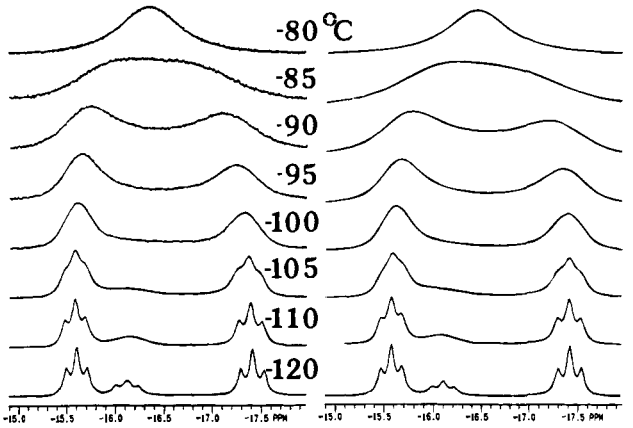

Figure 5. Observed (left) and calculated (right) variable-temperature ^{1}H NMR spectra (300 MHz) of the hydride resonances of $Os(H)_2Cl_2L_2$.

(Scheme 3) below −35 °C. Such a process therefore cannot be used to explain any mechanism observed to have an activation free energy lower than about 9 kcal/mol.

Isomerization in $OsH_2X_2L_2$. Figure 5 shows the ^{1}H NMR spectra of $OsH_2Cl_2L_2$ recorded between −80 and −120 °C in CD_2Cl_2 (5−10% of toluene-d_8 was added to lower the freezing temperature). These spectra are representative of all 'X_2' complexes in that the single OsH_2 triplet decoalesces into *three* resonances below −80 °C. Similarly, low-temperature ^{31}P NMR spectra exhibit three resonances (see below). No solvent (THF, toluene) dependence of coalescence is found when X = Cl, but there is some halide dependence: the decoalescence temperature decreases for each heavier X by 5−7°. The latter, in conjunction with a parallel *increase* in the separation of the decoalesced lines (X = Cl: 1.81 ppm; X = Br: 2.23 ppm; X = I: 2.97 ppm, for the outermost resonances), indicates acceleration of the exchange with increase of the halide atomic number. That is, the $\Delta G^{\ddagger}$ for rearrangement is smaller for the heavier halides. This study was extended to include an example with bulkier ligands, $Os(H)_2Cl_2(P^tBu_2Me)_2$, which proved to be a more simple case. The hydride resonance of $Os(H)_2Cl_2(P^tBu_2Me)_2$ remains a well-resolved triplet at −110 °C in CD_2Cl_2/toluene-d_8. This additionally supports the idea that the NMR observations for $Os(H)_2X_2(P^iPr_3)_2$ are not caused by hindered rotation of or within the phosphine ligands. Below we will discuss the VT ^{31}P NMR data for $Os(H)_2Cl_2(P^iPr_3)_2$, which also speak against this possibility.

The observation of three resonances (with relative intensities of 2, < 1, and 2) in the low-temperature ^{1}H NMR spectra of $OsH_2X_2L_2$ suggests that these complexes exist in two isomeric forms: 'symmetric' (**1-X_2**) with equivalent hydrides and 'nonsymmetric' (**2-X_2**) with nonequivalent H ligands.

To be in agreement with the above conclusion on the absence of direct pairwise hydride exchange in $OsH_2I_2L_2$ below −35 °C, we suggest the following dynamic model (Scheme 4) to explain averaging hydride environments in $OsH_2X_2L_2$ (δ values are given for the case X = Cl and *a* and *b* label nuclei, while *1*, *2*, and *3* label chemical shifts):

Using the DNMR5 program, this exchange model provides satisfactory agreement between the experimental and calculated spectra (Figure 5). As is often the case in dynamic NMR, the most reliable rate constants come from spectra recorded near the decoalescence temperature. For $OsH_2Cl_2L_2$, the simulation resulted in $\Delta G^{\ddagger}$ = 7.4 ± 0.1 kcal/mol between −80 and −90 °C.[32]

This discussion in terms of the exchange model presented above can be easily extended to a more general case when the

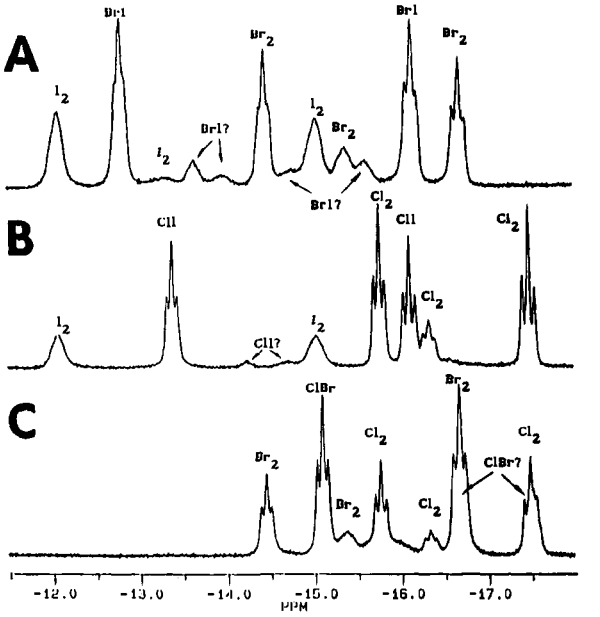

Figure 6. Low-temperature (−110 °C) ^{1}H NMR spectra (500 MHz) of the hydride resonances of equilibrium mixtures of (A) $Os(H)_2I_2L_2$, $Os(H)_2BrIL_2$, and $Os(H)_2Br_2L_2$; (B) $Os(H)_2I_2L_2$, $Os(H)_2ClIL_2$, and $Os(H)_2Cl_2L_2$; and (C) $Os(H)_2Br_2L_2$, $Os(H)_2BrClL_2$, and $Os(H)_2Cl_2L_2$.

Scheme 4

δ_1 -15.60; δ_2 -17.41; δ_3 -16.12

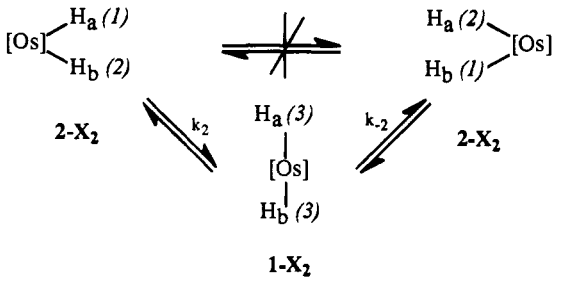

halides are not the same. Obviously, the chemical shifts in **1-XY** are then different (δ' and δ'') and the exchange results in *two* averaged chemical shifts, δ'_{av} and δ''_{av}, when $k_2 > k_1$ and $k_1 < (\delta'_{av} - \delta''_{av})\pi/\sqrt{2}$: δ'_{av}(or δ''_{av}) = $(\delta_1 + \delta_2)m/2 + n\delta'$ (or δ''), where *m* and *n* are mole fractions of **2-XY** and **1-XY**, respectively. This is the case for OsH_2BrIL_2 between −35 and −90 °C and for OsH_2ClIL_2 between −68 and −90 °C. It follows that $k_2 \approx k_1$ in OsH_2ClBrL_2 since these two different intramolecular dynamic processes become slow on the NMR time scale somewhat below −85 °C.

At this point, one additional important detail must be mentioned. Intuitively, one should expect that in a case of nonequivalent halides, the number of nonsymmetric isomers **2-XY** can be more than one. The extra resonances in the spectra presented in Figure 6 for all OsH_2XYL_2 support this idea, but certain isomer populations are too small for a quantitative analysis.[33]

Phosphine Exchange in 2. Inspection of the ^{1}H NMR spectra presented in Figures 5 and 6 reveals an important detail.

(32) We consider it unwise to discuss a temperature dependence of the determined rate constants (i.e., individual $\Delta H^{\ddagger}$ and $\Delta S^{\ddagger}$) because below −90 °C broadening caused by the exchange and fast spin−spin relaxation are comparable and cannot be rigorously separated in the present case.

(33) Independent of the number of isomers, the above conclusion predicting two resonances, products of **2-XY** ⇌ **1-XY** isomerization, remains valid.

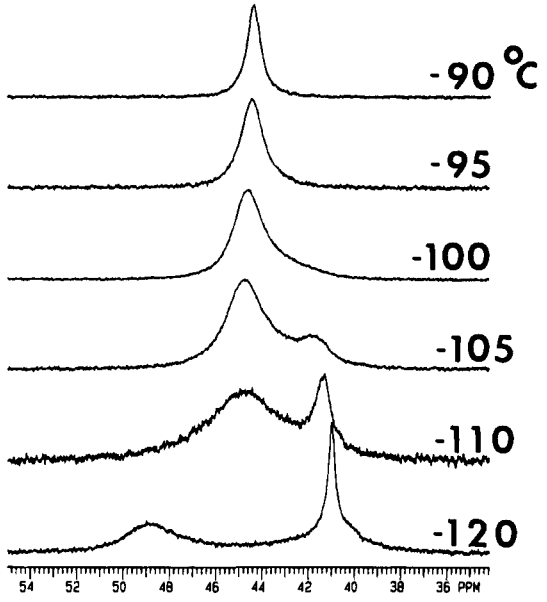

Figure 7. Variable-temperature $^{31}P\{^1H\}$ NMR spectra of $Os(H)_2Cl_2(P^iPr_3)_2$.

The decoalesced hydride resonances of **2** are *triplets* suggesting either (1) accidental equivalence of the phosphines or (2) an additional dynamic process operating to average the phosphorus nuclei. The latter idea finds confirmation in $^{31}P\{^1H\}$ NMR. It is clearly seen in Figure 7 that in **2**-Cl_2 the phosphines are in fast exchange well below the point when the isomerization **2**−**XY** ⇌ **1**-**XY** is spectroscopically slow. It is worth mentioning that the spectra shown in Figures 5 and 7 originate from the same sample, recorded at the same temperature using a ^1H/BB switchable probe. When the $^{31}P\{^1H\}$ NMR spectrum decoalesces, one observes one species with an AX pattern (more abundant) and a second with an M_2 spin system. Note that the nonsymmetric isomer is the more abundant one in both ^{31}P and ^1H NMR spectra.

Using the decoalescence temperature (about −115 °C) a rate constant k_3 can be estimated as $k_3 = \Delta\delta\pi/\sqrt{2} = 3.2 \times 10^3\ s^{-1}$ providing α $\Delta G^{\ddagger}$ value of 6.5 kcal/mol for the phosphine exchange between the two sites *within* the nonsymmetric isomer **2**-Cl_2. However, isomerization (site exchange) between the symmetric and nonsymmetric isomers has (Figure 7) an appreciably higher $\Delta G^{\ddagger}$ than 6.5 kcal/mol. Thus, k_3 represents a third fluxional process which makes the two phosphines equivalent within **2**-Cl_2.

It is possible to slow down these processes below −120 °C using a $CFDCl_2$−CF_2DCl mixture as a solvent. At the slow-exchange limit, reached at −140 °C, each resonance of **2**-Cl_2 is a doublet of doublets in both ^1H (hydride region) and hydride-coupled ^{31}P NMR. These spectra analyzed as those of an $H_aH_bP_aP_b$ spin system to give two independent sets of the coupling constants: $^2J(H_a-P_a) = 26[23]$ Hz, $^2J(H_a-P_b) = 37$-[34] Hz, $^2J(H_b-P_b) = 29[27]$ Hz, $^2J(H_b-P_a) = 41[40]$ Hz. The values in brackets are from ^{31}P NMR and can be less accurate if slightly affected by (presumably selective) decoupling. No evidence was found for a detectable P_a-P_b coupling, which is in agreement with the magnitude (≪ 14 Hz) predicted above from the ^1H NMR data. The H_a-H_b coupling is also small, as revealed by homonuclear decoupling at −120 °C. Irradiating at δ H_b reduced the line width of the H_a resonance by only 3 Hz.

One important conclusion can be made about the signs of the proton-phosphorus couplings. The sums, $|^2J(H_a-P_a) + {}^2J(H_a-P_b)|$ and $|^2J(H_b-P_a) + {}^2J(H_b-P_b)|$, are given by the separation of the outermost lines of the hydride multiplets and are found to be independent of the exchange rate k_3. This observation requires identical signs for the coupling constants in brackets.

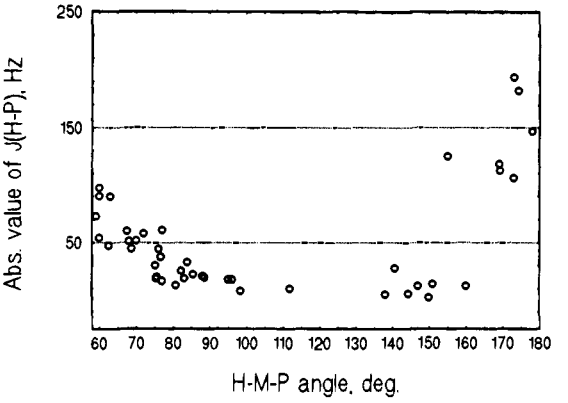

Figure 8. Dependence of ^2J(H−M−P) on the H−M−P angle for the complexes listed in Table 1.

H−M−P Angle Dependence for ^2J(H−P) and Possible Structure of 2-X_2. It is well-known that in metal hydrides *cis* ^2J(H−P) couplings are typically between 15 and 30 Hz and there is some evidence for a negative sign of the couplings. In contrast, a positive sign is associated with large (up to 180 Hz) *trans* ^2J(H−P) constants. In all those cases, the H−M−P angles are probably not very different from 90° and 180°, respectively.[34]

In order to better comprehend the angular dependence of ^2J(H−P), we collected (supplementary material) reported coupling constants accompanied by structural information. These data are represented graphically in Figure 8 as $|^2J(H-P)|$ vs the H−M−P angle, α.

Based on the results plotted in Figure 8, some conclusions can be made with confidence.[35] Available data indicate a flatness between 90° and 140° followed by a strong increase of the coupling when α > 140°. ^2J(H−P) also increases when α falls below 90°, and changes sign at *ca.* 75−80°. This phenomenon is particularly evident in complexes with a four-legged piano-stool geometry where the *cis* couplings (α ≤ 80° are *greater* than *trans* values (α ≥ 90°). An example of this behavior is $[(\eta\text{-}C_5H_5)Ir(PMe_3)(H)_3]^+$ where α(*trans*) = 98° and α(*cis*) = 75°. The coupling constants reported for $[(\eta^5\text{-}C_5H_5)Ir(PPh_3)(H)_3]^+$ are ∓8.3 Hz (*trans*) and ±16 Hz (*cis*).[36]

A better understanding and accuracy for the ^2J(H−P) vs α dependence should come with new spectroscopic and structural data. Important insights might also be provided by theoretical calculations.

With this information in mind, it seems reasonable to conclude that rather large (37−41 Hz) ^2J(H−P) values in **2**-Cl_2 are most probably positive and result from a molecular geometry distorted from ideal octahedral. Based on the available data, the couplings in **2**-Cl_2 suggest either ∠H−Os−P ≤ 90° or 140° < ∠H−Os−P < 180°. Under all the constraints, the easiest way to construct a molecular structure for **2**-Cl_2 is to start from the symmetric isomer and move one of the hydrides to a PClCl face; moderate movement of the Cl_2P_2 substructure is also possible (Scheme 5).

(34) (a) Benn, R.; Joussen, E.; Lehmkuhl, H.; López Ortiz, F.; Rufińska, A. *J. Am. Chem. Soc.* **1989**, *111*, 8754. (b) Eisenschmid, T. C.; McDonald, J.; Eisenberg, R.; Lawler, R. G. *J. Am. Chem. Soc.* **1989**, *111*, 7267.

(35) $HRe(PMe_3)_5$ is one example with exceptional coupling constants. In particular, $J(P-H_{cis})$ is larger than $J(P-H_{trans})$. See: Jones, W. D.; Maguire, J. A. *Organometallics* **1987**, *6*, 1728.

(36) Heinekey, D. M.; Millar, J. M.; Koetzle, T. F.; Payne, N. G.; Zilm, K. W. *J. Am. Chem. Soc.* **1990**, *112*, 909.

Table 1. Enumeration of the 12 Isomeric Subgroups of $Os(H)_2Cl_2(PH_3)_2$ Described in the Text

	[2] substructure											
	HH		ClCl		$(PH_3)(PH_3)$		HCl		$H(PH_3)$		$Cl(PH_3)$	
[4] substructure	cisoid	transoid	cisoid	transoid	cisoid	transoid	cisoid	transoid	cisoid	transoid	cisoid	transoid
subgroup	[*c*,HH]	[*t*,HH]	[*c*,ClCl]	[*t*,ClCl]	[*c*,PP]	[*t*,PP]	[*c*,HCl]	[*t*,HCl]	[*c*,HP]	[*t*,HP]	[*c*-ClP]	[*t*,ClP]

Scheme 5

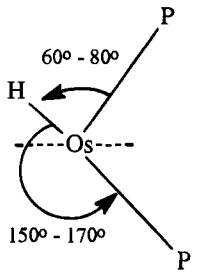

Given these experimental observations (i.e., both the conclusive results and those, such as the nonsymmetric isomer, requiring additional structural definition), we chose to perform an *ab initio* study on the $OsH_2Cl_2(P^iPr_3)_2$ system, modeled by $OsH_2Cl_2(PH_3)_2$, with the following goals: (1) to propose likely structures for both the symmetric and especially the nonsymmetric isomers of $OsH_2Cl_2(P^iPr_3)_2$, (2) to understand the origin of the unusual solid-state geometry,[1] and (3) to use the structure and bonding of calculated structures to further describe the various fluxional processes.

Computational Results

Strategy and General Studies. Due to the general difficulty of finding stationary points for systems having a large number of degrees of freedom, $OsH_2Cl_2(PH_3)_2$ presented a challenge for computational studies. To approach this problem, we felt it necessary to first devise a strategy for locating regions of the potential energy surface (PES) where minima are likely to be found. Both the solid-state structure of $OsH_2Cl_2(P^iPr_3)_2$ **1** and the structures of other $ML_2L'_2L''_2$ systems[37] were used to determine a reasonable starting point for our investigation. Each of these structures consists of a grossly distorted octahedron in which two of the *trans* ligands are distorted toward each other, resulting in either C_2 or C_{2v} symmetry. While it is possible to view these structures as distorted octahedra, there are also other possible geometric descriptions. Because of the difficulty in uniquely describing the geometry of these complexes as derived from regular polyhedra, we have chosen to describe them as [4]/[2] molecules, indicating that when the molecule is divided by a plane through the metal and perpendicular to the C_2 (or pseudo-C_2) axis, there are four ligands on one side of the plane and two on the other. By rotation of the [2] substructure with respect to the [4] substructure, the full variety of observed isomers for this type of system can be obtained.

For three different pairs of ligands (H_2, Cl_2, and $(PH_3)_2$ in this system), there are six different [4]/[2] groups, since the ligands within the [2] substructure are not necessarily identical. We will label these six groups by the identity of the atoms of the [2] substructure bound to osmium, i.e., HH, ClCl, PP, HCl, HP, and ClP. Since each set of ligands of the [4] substructure contains at least one pair of identical ligands, the six major groups can be further divided into subgroups based on the relationship between the identical ligands within the [4] substructure. Each subgroup is labeled either [*c*] for cisoid or [*t*] transoid depending upon their relationship when viewed down the C_2 (or *pseudo* C_2) axis. Within each of the twelve subgroups there is an infinite set of rotamers possible based upon the relationship of the [2] substructure to the [4] substructure. The derivation of the groups and subgroups for this system is given in Table 1. Figure 9 shows examples of this labeling method on $MX_2Y_2Z_2$. In this figure, the first pair of molecules are two of the infinite number of rotamers from the [*t*,XX] subgroup, having two X ligands in the [2] substructure, with both the Y and Z ligands of the [4] substructure transoid. Each of these rotamers is given the same name as they are part of the same subgroup. The third molecule shown belongs to the [*c*,XY] subgroup as there is one X and one Y in the [2] substructure and the Z ligands of the [4] substructure are cisoid.

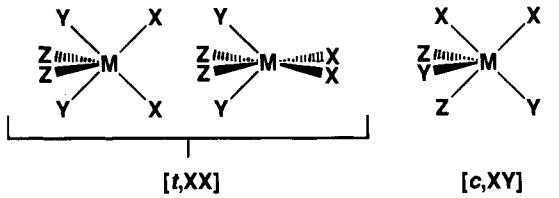

Figure 9. Examples of the labeling scheme used for $MX_2Y_2Z_2$ molecules. See text for discussion.

Since the phosphines used in experimental studies are bulky, the subgroups having a cisoid arrangement of the two phosphines in the more crowded positions of the [4] substructure ([*c*,HH], [*c*,ClCl], and [*c*,HCl]) were not considered for any calculations. Even after this process of elimination, however, there are nine remaining subgroups to be investigated, each having a full set of rotamers.

In order to approach this problem in an efficient manner, we chose to first explore the three most symmetric subgroups of isomers: [*t*,HH], [*t*,ClCl], and [*t*,PP]. The two different rotamers having the ligands of the [2] substructure eclipsing the ligands of the [4] substructure were examined for each subgroup, giving a total of six isomers. Each of these isomers was optimized at the MP2 level with constrained C_{2v} symmetry. The results of these optimizations are presented in Table 2. With these results and general concepts of steric effects, the following approaches were used to select the best subgroups for the symmetric and nonsymmetric isomers:

(a) Approach to the Symmetric Isomer. The lowest energy structure of our initial study was found in the [*t*,ClCl] subgroup. This is important because it is from this group that the solid-state structure of $OsH_2Cl_2(P^iPr_3)_2$ is derived. Since the [*t*,ClCl] subgroup has C_2 symmetry for all rotamers, this subgroup was chosen as a starting point for study of the symmetric isomer.

(b) Approach to the Nonsymmetric Isomer. A more thorough examination of the initial study was necessary to choose a reasonable starting point for our investigation of the nonsymmetric isomer. The two structures of the [*t*,PP] subgroup were found to be significantly higher in energy than either the [*t*,HH] or [*t*,ClCl] subgroups (Table 2). This alone led us to rule out the entire [PP] group ([*c*,PP] and [*t*,PP]) in further studies. In addition, we observed that the ligand−Os−ligand angles of the [2] substructure in the optimized structures were invariably small (52.6° to 88.3°). It would seem that in the actual system with bulky phosphines, any geometry having even one phosphine in the [2] substructure would thus be disfavored,

(37) Kubáček, P.; Hoffmann, R. *J. Am. Chem. Soc.* **1981**, *103*, 4320.

Table 2. Relative Energies of Structures Considered

	Relative E (kcal/mol)	Cl-Os-Cl (°)	P-Os-P (°)	H-Os-H (°)
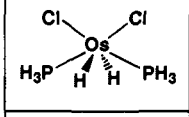	0.00	88.3	111.7	111.5
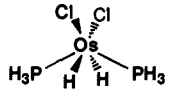	16.9	83.0	96.4	123.2
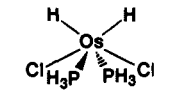	7.7	144.5	183.6	60.1
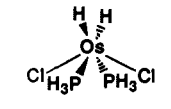	31.4	165.4	173.3	52.6
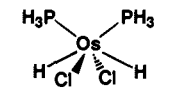	62.0	157.4	82.2	152.1
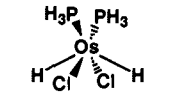	90.1	123.7	74.5	168.7

and so we also did not pursue any structure having one phosphine in a position of the [2] substructure (eliminating [*c*,HP], [*t*,HP], [*c*,ClP], and [*t*,ClP]). Of the remaining three subgroups [*t*,HH], [*t*,ClCl], and [*t*,HCl], only the [*t*,HCl] subgroup could readily provide a structure that was nonsymmetric, and so further studies on a nonsymmetric isomer were performed on this subgroup.

The Symmetric Isomer. For the reasons described above, the [*t*,ClCl] subgroup was chosen for studies of the symmetric isomer of $OsH_2Cl_2(PH_3)_2$. Optimization of the lowest energy structure from our initial study (the rotamer having the Cl−Os−Cl plane eclipsing the P−Os−P plane) with no symmetry constraints at both the RHF and RHF/MP2 levels produced virtually identical results, and as a result, RHF level calculations were used for the remainder of this section. The rotamers in this subgroup are defined by the dihedral angle between the Cl−Os−Cl and P−Os−P planes (ω), where $\omega = 0°$ is the structure described having the Cl−Os−Cl plane eclipsing the P−Os−P plane.

Having optimized the $\omega = 0°$ rotamer (**M1**, where **M** designates model compound, with PH_3 as the phosphine), the $\omega = 90°$ rotamer (**M2**) was then optimized with no symmetry constraints, and this geometry was also found to be an extremum at 20.8 kcal/mol above **M1**. Other than the difference in ω, the geometric parameters calculated for the two structures are very similar, with the greatest difference occurring in the two P−Os−P angles (111.2° for **M1** *vs* 102.2° for **M2**). Drawings of the optimized structures of **M1** and **M2** with selected distances and angles are shown in Figure 10, parts a and b, respectively. Since the solid-state structure of $OsH_2Cl_2(P^iPr_3)_2$ is from this same subgroup, but with $\omega = 45°$, the PES of our model complex was investigated for $0° \leq \omega \leq 90°$ using average bond lengths and angles from **M1** and **M2**. As shown in Figure 11a, $\omega = 90°$ was calculated to be the highest energy rotamer (now 20.9 kcal/mol above $\omega = 0°$), and the $\omega = 45°$ rotamer was only 8.8 kcal/mol above $\omega = 0°$. These results clearly indicate that the $\omega = 0°$ rotamer (**M1**) is the preferred geometry for the symmetric $OsH_2Cl_2(PH_3)_2$.

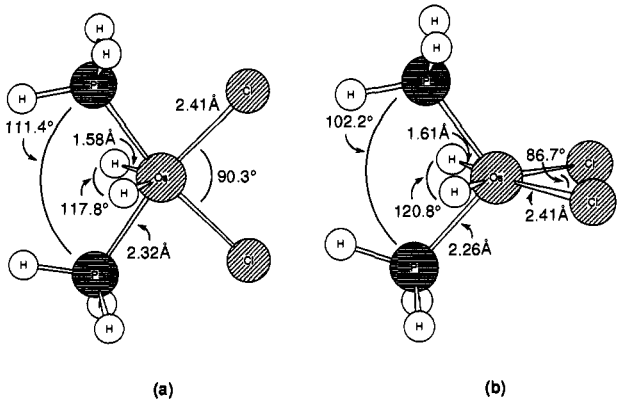

Figure 10. Distances and angles for two RHF optimized structures (**M1** and **M2**) of $Os(H)_2Cl_2(PH_3)_2$. Views are perpendicular to the C_2 axis.

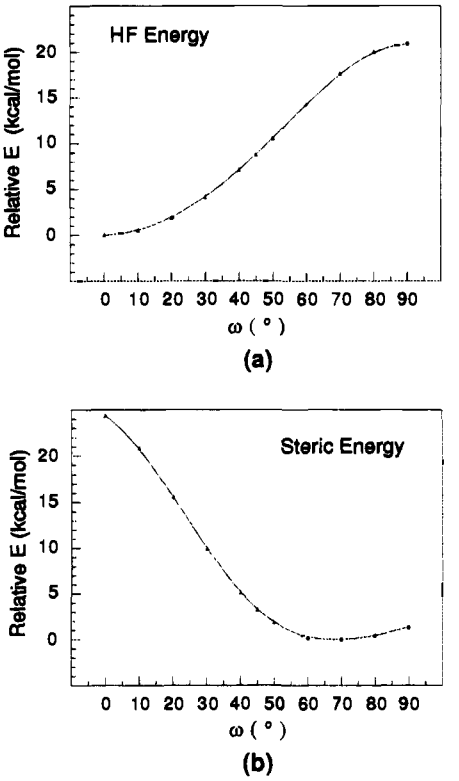

Figure 11. (a) Hartree−Fock energy profile of $Os(H)_2Cl_2(PH_3)_2$ and (b) molecular mechanics energy profile of $Os(H)_2Cl_2(P^iPr_3)_2$ during rotation of the $OsCl_2$ plane relative to the OsP_2 plane (coplanar has $\omega = 0°$).

There are two important points to note from these results: (1) the minimum energy structure is found to be non-octahedral and (2) **M1** is significantly more stable than **M2**, showing that the heavy atoms do not prefer the pseudo-tetrahedral heavy-atom skeleton which would minimize phosphorus/chlorine steric interactions. From previous studies on both $OsH_3Cl(PH_3)_2$ and $OsHCl_3(PH_3)_2$,[15a] it was shown that, in these unsaturated systems, distortion away from an octahedron is associated with the need to maintain a diamagnetic state for a d^4 electron count. In addition, the distortion also enhances π bonding between the electron-deficient metal and a π-donor ligand. To assess the importance of similar factors in the bonding of $OsH_2Cl_2(PH_3)_2$, the interaction between selected fragment molecular orbitals of

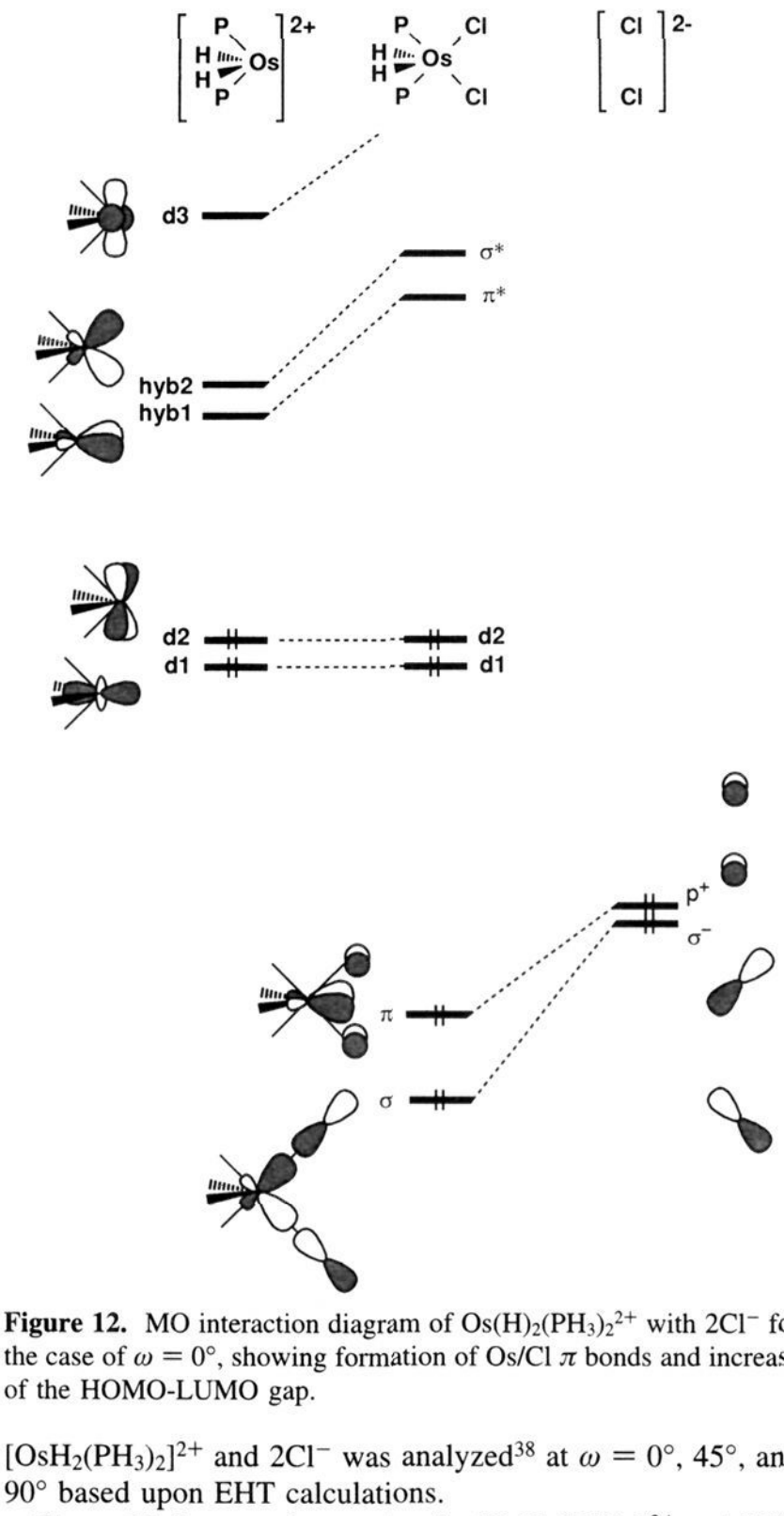

Figure 12. MO interaction diagram of $Os(H)_2(PH_3)_2^{2+}$ with $2Cl^-$ for the case of $\omega = 0°$, showing formation of Os/Cl π bonds and increase of the HOMO-LUMO gap.

$[OsH_2(PH_3)_2]^{2+}$ and $2Cl^-$ was analyzed[38] at $\omega = 0°$, 45°, and 90° based upon EHT calculations.

Figure 12 shows an interaction for $[OsH_2(PH_3)_2]^{2+}$ and $2Cl^-$ in the $\omega = 0°$ rotamer, though this drawing is valid for representing the interaction in any eclipsed [4]/[2] system. It should first be noted that the large HOMO-LUMO gap, which is necessary to maintain a diamagnetic state, can be attributed to the geometry of the [4] substructure, regardless of the orientation of the [2] substructure. The $[OsH_2(PH_3)_2]^{2+}$ fragment has five metal-based frontier orbitals which fall into three groups: (1) filled metal−ligand nonbonding orbitals (labeled **d1** and **d2**), (2) empty σ antibonding orbitals which are hybridized away from the [4] substructure (labeled **hyb1** and **hyb2**), and (3) an empty, completely σ antibonding orbital (labeled **d3**). Not shown are the higher energy σ hybrid orbitals having s, p, and d character. The σ^- combination of the chlorides forms a σ bond with **hyb2** while the σ^+ combination (not shown) interacts with the high-energy metal σ hybrid (also not shown). The **hyb1** orbital is ideally suited to form a π interaction with p^+ (p^- is not shown since it does not interact significantly with the metal d orbitals). The result is a π-stabilized complex as was found for both $OsH_3Cl(PH_3)_2$ and $OsHCl_3(PH_3)_2$. We find that rotation of the chlorides causes mixing of **d1** and **d2** to retain two nonbonding orbitals and mixing of **hyb1** and **hyb2** to provide a pair of empty orbitals, one of which is used for a σ-type bond and the other for a π-type bond. Thus, each rotamer maintains a large HOMO-LUMO gap, Cl/Os σ bonds, and an effective Cl/Os π interaction. While a similar π interaction is possible for structures having the chlorine atoms in the [4] substructure (i.e., [*t*,PP] and [*t*,HH]), it is found to be of a lesser magnitude. This difference is in part responsible for the preference for chlorine atoms in the [2] substructure.

Because each rotamer of $OsH_2Cl_2(PH_3)_2$ is able to provide π density to the metal, the preference of **M1** over **M2** must not be due to the π bonding. In fact, σ effects dominate the difference in energy between the two structures. As also shown in our study of $OsH_3X(PR_3)_2$, hydrides are preferentially *trans* to an empty space as a result of their very large *trans* effect. This same phenomenon is apparent in the dichloro case where the most stable conformation has the two chlorine atoms *trans* to the phosphines rather than to the hydrides.

As neither σ nor π effects are responsible for the intermediate structure of the observed $\omega = 45°$ geometry, steric effects from the bulky phosphine ligands must play a role in the experimental system. The placement of the chlorine ligands is the outcome of two opposing forces: (1) the hydrides, because of their strong σ-donating ability, are directing the chlorines to be *trans* to the phosphines, and (2) the phosphines, because of their steric bulk, are pushing the chlorines to be *trans* to the hydrides. We have attempted to simulate these steric effects by replacing PH_3 with P^iPr_3 and estimating the steric energy as a function of ω using a molecular mechanics program. At each angle ω, the conformation of each phosphine was optimized. The steric energy is minimum for $\omega = 70°$ and maximum for $\omega = 0°$ (Figure 11b). While we cannot directly compare the energies obtained by the two methods (i.e., Figure 11, parts a and b), it is nevertheless remarkable that the *ab initio* energy varies less from $\omega = 0$ to 45° than above 45° while the steric energy does the opposite. Clearly the observed structure ($\omega = 45°$) represents a compromise between these two factors.

The Nonsymmetric Isomer. For the reasons described above, the [*t*,HCl] subgroup was chosen as the most likely source of a nonsymmetric isomer of $OsH_2Cl_2(PH_3)_2$. That is, this subgroup seemed to offer the best starting point for a search of the optimum nonsymmetric structure. Indeed, starting from a variety of possible rotamers in this subgroup, a single structure was obtained. To facilitate optimization, the P−Os−P and H(2)−Os−Cl(4) planes of the [4] substructure were held perpendicular during optimization, though no other constraint was imposed (i.e., Os−P distances were not required to be identical, etc.).[39] The resulting structure (**M3**) optimized (MP2) to a stationary point at 22.2 kcal/mol above **M1**. Two views of the structure of **M3** are shown in Figure 13.

The geometry of **M3** is quite unusual. The phosphines, and thus the hydrogen and chlorine, of the [4] substructure of **M3** are in the transoid arrangement, but the ligands of the [2] substructure are substantially distorted from the geometries seen previously. In all previously-described molecules, the ligands of the [2] position are related by a pseudo-C_2 axis. In **M3**, however, this relationship is no longer present. In fact, H(3), P(6), and P(7) are coplanar while Cl(5) lies nearly in the perpendicular H(2)−Os(1)−Cl(4) plane.

Inspection of the molecular orbitals of **M3** shows that this unusual arrangement of the [2] substructure does very little to alter the important features of the bonding scheme shown in

(38) The frontier molecular orbitals of the OsL_4 fragment are readily derived qualitatively as in: Albright, T. A.; Burdett, J. K.; Whangbo, M.-H. *Orbital Interactions in Chemistry*; Wiley: New York, 1985; Chapter 19.

(39) Release of this constraint produced no significant change in either the geometry or energy of the complex.

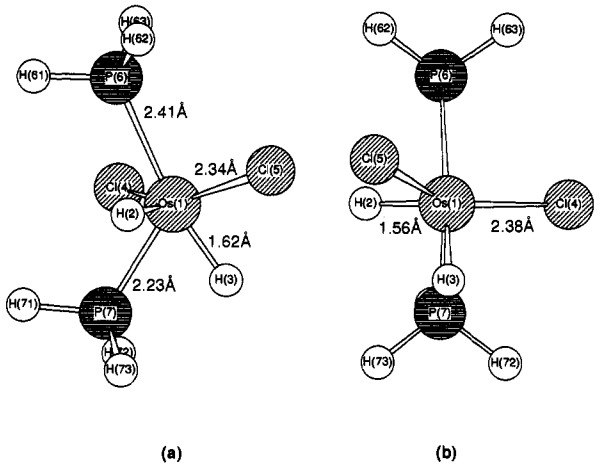

Figure 13. Two views of the MP2 optimized geometry of the **M3** isomer viewed perpendicular (left) and edge-on (right) to the OsP_2 plane.

Figure 12. As before, we find a well-separated HOMO and LUMO, with the two highest energy, filled metal-based orbitals being nonbonding with respect to all ligands. In the [*t*,ClCl] rotamers, a σ bond from Os to the ligands of the [2] substructure was formed using only one of the empty, low-energy metal-based orbitals of the OsL_4 fragment (**hyb2**), thus leaving the other empty, low-energy metal-based orbital (**hyb1**) for π bonding. In **M3**, each of the two empty, low-energy metal-based orbitals of the OsL_4 fragment is used to form a σ bond to one of the two ligands of the [2] substructure. This bonding is increased by mixing of the high-lying σ hybrid orbital into the two σ bonds. In addition, the LUMO of **M3** is the π antibonding orbital that results from the formation of a filled π bonding interaction with the chlorine atoms. Unfortunately, complicated orbital mixing obscures the source of the metal-based π orbital. Unlike the symmetric systems, the Os−Cl π interactions are not the same for the two chlorines as reflected in the different Os−Cl bond lengths. As there is no molecular symmetry, the two Os−P and the two Os−H bond lengths are also notably different, with the P and H atoms *trans* to one another showing lengthened Os−P and Os−H bonds.

While **M3** is much higher in energy than **M1** when PH_3 is the phosphine, we believe that **M3** is still a reasonable suggestion for the nonsymmetric isomer observed for $OsH_2Cl_2(P^iPr_3)_2$. As with the symmetric isomer, the poor representation of P^iPr_3 by PH_3 is the cause of the energy discrepancy.[40] **M3** exhibits two sources of steric relief as compared to **M1**. First, the calculated P−Os−P angle is much larger in **M3** than in **M1** (125.3° *vs* 111.2°). This larger angle alleviates steric congestion that is present in **M1**. Even more significant is that the Os−Cl(5) vector lies 62° out of the Os−P(6)−P(7) plane in **M3** as compared to eclipsing the Os−P(6) bond in **M1**. This difference should also provide important relief of steric crowding in **M3**. It should also be noted that the molecular mechanics minimum calculated for this dihedral angle was 70°. Both of these differences will significantly decrease the 22.2 kcal/mol energy difference calculated between **M1** and **M3** in the direction of the very small difference observed between the symmetric and nonsymmetric isomers of $OsH_2Cl_2(P^iPr_3)_2$.

Merging the Experimental and Computational Results

The NMR studies described here demonstrate that in solution $OsH_2Cl_2(P^iPr_3)_2$ exists in two isomeric forms: one isomer shows equivalence of both H and P nuclei at low temperature, while the other isomer shows inequivalence of both H and P nuclei at low temperature. A variety of fluxional processes have been observed for these two isomers including interconversion of the two isomers and a process of P site-exchange within the nonsymmetric isomer. An additional fluxional process has been detected in the symmetric isomer by incorporating two different halides.

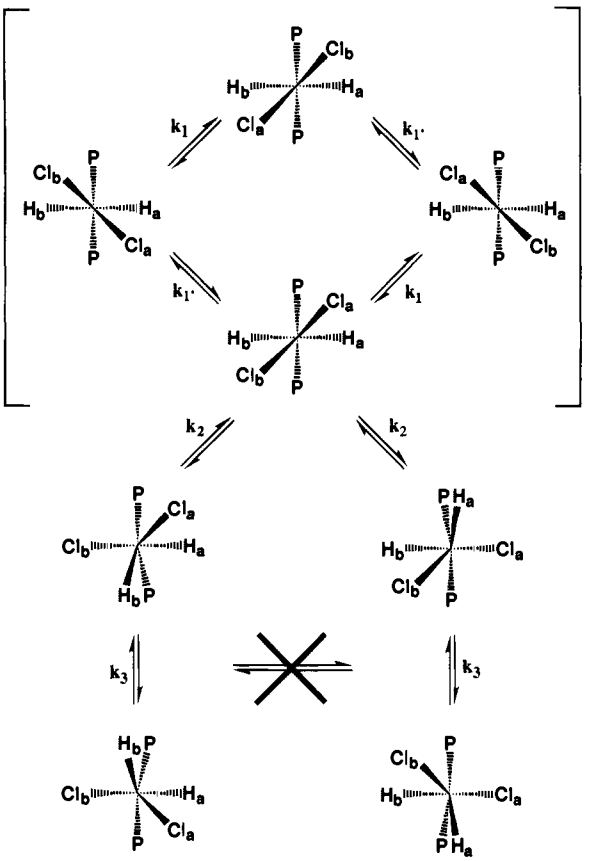

Figure 14. Mechanistic scheme for rearrangements observed among $Os(H)_2XY(P^iPr_3)_2$ molecules.

The calculated structures **M1** and **M2**, as well as the solid-state structure of $OsH_2Cl_2(P^iPr_3)_2$, are in agreement with the spectral data for the symmetric isomer. Further, we find that the solid-state structure can be understood as a conflict between P^iPr_3−Cl steric and Cl−Os bonding preferences. Such conflict allows the facile rotation of the halides (see Scheme 3), which can only be detected when there are non-identical halides in the molecule.

Establishing the structure of the nonsymmetric isomer must rely on computational evaluation of plausible candidates. However, it should be especially noted that the NMR data were used to estimate angles of <90° and 140−170° for H−Os−P in the nonsymmetric isomer, and the calculated values of these angles in **M3** are 65.8° and 168.7°, respectively. This agreement in angles, along with the steric relief provided by this geometry (*vide supra*), supports the viability of **M3** as the structure of the nonsymmetric isomer.

Using this information, we are able to propose a mechanism for the fluxional processes observed. Figure 14 shows two physical mechanisms which can account for the dynamic NMR phenomena: the **2-X$_2$** ⇌ **1-X$_2$** isomerization (k_2) and phosphine site exchange within **2-X$_2$** (k_3). Both of them can be described as face-to-face migration of the hydride (and halide!) ligands within a distorted MX_2L_2 tetrahedron.[41] The lowest energy process (k_3) has one hydride "jump" (traverse) an X/X edge

(40) The energy difference in the experimental system must be small (<1 kcal/mol) as the two isomers are seen in similar amounts.

(with structural adjustments elsewhere in the structure). This accomplishes site exchange between inequivalent phosphorus sites. The next higher energy motion is H jumping a P/X edge, which isomerizes **1** and **2** (as seen by ^1H and ^{31}P NMR spectroscopy). Finally, a still more highly energetic motion for the heavier halides, and one which generates no higher symmetry, is a twisting of the OsX_2 triangle through the OsP_2 plane, which is detected only in the lower symmetry OsH_2XYP_2 series.

Conclusions

The molecules $Os(H)_2XY(P^iPr_3)_2$ have been synthesized by a new halide exchange reaction which is unusual for its selectivity (i.e., leaves the hydrides untouched). The unsaturation of these molecules is equally well demonstrated by the observed redistribution between $Os(H)_2X_2L_2$ and $Os(H)_2Y_2L_2$ species. All of these undergo an especially rich variety of fluxional processes whose rapid rates are unusual for coordination number six.

It should be recognized that the experimentally determined structure (Figure 1) of $Os(H)_2Cl_2(P^iPr_3)_2$ in fact closely conforms to a trigonal prism, **4** (when allowance is made for the size

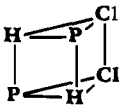

4

difference between H and P^iPr_3), which indeed has the requisite C_2 symmetry (and also has the symmetry of a "square antiprism with two missing vertices", as preferred in ref 1). The trigonal prism description also clearly is consistent with and underlies our [, XY] notation. This description can also be adapted to the processes k_1, k_2, and k_3 in Figure 14, where each k_1 rearrangement is a 90° rotation of a pair of eclipsed ligands (e.g., chlorides), one from each triangular face of the trigonal prism. However, it should be noted that there is no electronic preference for a trigonal prism, which is preferred instead for d^0 and d^2 electron counts.[4] The actual shape of $Os(H)_2X_2(P^iPr_3)_2$ results from a compromise between electronic and steric effects. In addition, the other isomeric structure (**M3**) has no symmetry, frustrating an objective determination of whether it is better "described" as derived from the *alternative* trigonal prism **5** or as a bicapped tetrahedron. No conclusion in this paper would be altered by adopting the trigonal prismatic terminology, vis-à-vis the bicapped tetrahedron.

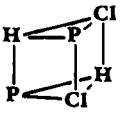

5

The molecules $Os(H)_2X_2(P^iPr_3)_2$ represent a class with remarkable structural complexity and deviation from the octahedral form so common for coordination number six. The primary distortion away from octahedral geometry results from the need to maintain a diamagnetic state for this d^4 species. This effect is augmented by the formation of a π system between the electron-deficient metal center and the halide ligands. Further distortions arise from a competition between steric hindrance and *trans* effects. These molecules thus confirm and extend our proposal[42] that the frequent occurrence of "unsaturated" (ignoring halide π-donation) hydride compounds when at least one halide (X) ligand is present is due to X → M π-donation. There is ample evidence that such π-donation can influence the metal coordination polyhedron adopted (e.g., $IrX(H)_2L_2$[3]), but it has never before been demonstrated to cause such a grossly distorted shape or the coexistence of two isomers the way it does in $Os(H)_2X_2L_2$.[43] Moreover, as we have argued in other situations, this ground-state π donation still leaves the molecule "operationally unsaturated" (e.g., capable of adding donor molecules such as MeI).

Acknowledgment. The Laboratoire de Chimie Théorique is associated with the CNRS (URA 506) and is a member of ICMO and IPCM. This work has been supported by the U.S. NSF and by an international CNRS/NSF grant for U.S./France scientific collaboration. We thank IDRIS for a generous allocation of computer time. J.R.R. thanks the Ministère des Affaires Etrangères for a postdoctoral position. R.K. is grateful for an NSF Graduate Fellowship. We thank Stuart Macgregor and Eric Clot for discussion and technical assistance and Professor J. Gajewski for making us aware of the GEAR program.

Supplementary Material Available: Lists of Cartesian coordinates for **M1** and **M2** (RHF optimization), and **M1** and **M3** (RHF/MP2 optimization) details of the kinetic analysis, and references to compounds in Figure 8 (8 pages). This material is contained in many libraries on microfiche, immediately follows this article in the microfilm version of the journal, and can be ordered from the ACS; see any current masthead page for ordering information.

JA942531R

(41) This kind of reorientation was first described more than 20 years ago (where it was termed "tetrahedral tunneling") in complexes with a pseudotetrahedral arrangement of four phosphine ligands, MH_2L_4 (M = Fe, Ru). See: Meakin, P.; Muetterties, E. L.; Tebbe, F. N.; Jesson, J. P. *J. Am. Chem. Soc.* **1971**, *93*, 4701. Meakin, P.; Muetterties, E. L.; Jesson, J. P. *J. Am. Chem. Soc.* **1973**, *95*, 75. Isomer **2** is crudely the analog of *trans*-MH_2L_4 and **1** is likewise the analog of *cis*-MH_2L_4, when the reduction in symmetry from L_4 to L_2X_2 is taken into account.

(42) Caulton, K. G. *New J. Chem.* **1994**, *18*, 25.

(43) Other distortions of d^4 $ML_2L'_2L''_2$ complexes have been analyzed.[37]